

Core-level spectroscopic study of the evolution of the sulfur-passivated InP(001) surface during annealing

Z. Tian

Institute for Microstructural Sciences, National Research Council, Ottawa, Canada K1A 0R6

and Département de Physique et Groupe de Recherche en Physique et Technologie des Couches Minces (GCM), Université de Montréal, Case Postale 6128, Succursale Centre-Ville, Montréal, Québec, Canada H3C 3J7

M. W. C. Dharma-wardana* and Z. H. Lu

Institute for Microstructural Sciences, National Research Council, Ottawa, Canada K1A 0R6

R. Cao

Stanford Synchrotron Radiation Center, Stanford, California 94309-0210

L. J. Lewis

Département de Physique et Groupe de Recherche en Physique et Technologie des Couches Minces (GCM), Université de Montréal, Case Postale 6128, Succursale Centre-Ville, Montréal, Québec, Canada H3C 3J7

(Received 5 September 1996)

Core-level photoemission spectroscopy and theoretical predictions of structure and spectra are used to study the fully S-covered InP(001) surface and its evolution during annealing. The theory predicts a number of stable structures besides the lowest-energy ground state which is the fully S-covered (2×2) -reconstructed structure, where the surface has two types of S atoms. On annealing, a fascinating sequence of structures unfolds from the fully S-covered ground state as the other stable structures become energetically accessible. The surface S atoms exchange with bulk P atoms on annealing, forming new strong S–P bonds while dissociating preexisting S–S dimers. The S–P bonds are tilted with the P atoms just above the surface and there is only one type of S atom in the structure. The measured excitation energies and spectra agree with theoretical predictions of the core-level spectra for the (2×2) reconstruction and its evolution to partial S coverages. We conclude that the annealed surface around 700 K is most likely to be a (2×2) reconstructed surface with the surface cell containing two S–P bonds, with just one type of S atom. [S0163-1829(97)01308-8]

I. INTRODUCTION

High-resolution photoemission experiments measure core-level positions of atomic lines which shift as a function of the chemical environment of the atoms. Thus, core-level (CL) spectroscopy has become an important technique for distinguishing an atom in different bonding environments.¹ The method is a powerful tool for surface-structure elucidation when used with theoretical predictions of the CL excitation (CLE) energies for different “competing” structures. Competing structures may be relevant because the surface is not well understood, or because annealing, surface preparation, etc., may generate other structures besides the ground state. We present here studies of CLE and annealing of the sulfur-passivated InP(001) surface for which a (2×2) reconstruction has recently been proposed.² The topic is of wide interest given the innovative use of CL spectroscopy and theory to study annealing, and also technologically, since sulfur overlayers passivate III-V surfaces.^{3–5}

The “as-prepared” InP(001)-S surface was studied by Jin *et al.*² theoretically, using density-functional total-energy minimization methods,⁶ and experimentally, using Raman spectroscopy. The fully relaxed, lowest-energy ground state is the (2×2) structure of Fig. 1; this is also shown schematically in Fig. 2(a).

This structure is insulating and satisfies the electron

counting rule. The surface has two S sublayers separated by 0.335 Å. The top S sublayer contains monomer pairs separated by 3.82 Å, and close to bridge sites. The lower sublayer contains S pairs strongly dimerized along the $[\bar{1}10]$ direction, separated by 2.14 Å. Thus the S atoms exist in *two types of chemical environments* in Fig. 1.

A (2×1) reconstruction has been observed in photoemission and low-energy-electron-diffraction (LEED) studies of *annealed* samples by Mitchell *et al.*⁷ In this context, they considered the structure of Fig. 2(b), containing S dimer rows, and pointed out that it violated the electron counting rule. Our calculation of the total energy and forces for Fig. 2(b) shows it to be unstable (i.e., not even an energy minimum). However, *local* energy minima exist, e.g., Fig. 2(c), which has just one type of S atoms.² The energy of Fig. 2(c) is ~ 0.07 eV per S atom higher than that given by Fig. 2(a) (or Fig. 1). Such higher-energy structures become thermodynamically accessible on annealing. Also, the exchange of surface S atoms with bulk P atoms is promoted by annealing. The net effect of such exchanges is to replace the S atoms on the surface by P atoms, forming reconstructions, while the sulfur atoms diffuse into the bulk. Further heating leads to the totally S-free, P-rich, InP(001) surface. Our preliminary calculations and other studies of this surface suggest a (2×4) reconstruction;⁸ a detailed study of it is outside the

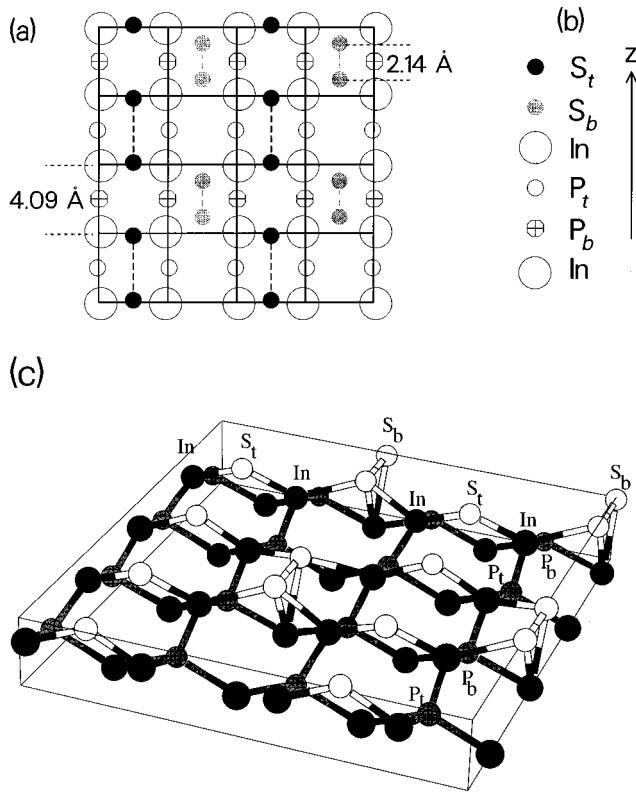


FIG. 1. (a) Top view of the fully relaxed, fully S-covered InP(001) surface. The atom species are identified in the z -direction ([001]) layer sequence shown in (b) and also in Eq. (1). The x and y directions are $[110]$ and $[\bar{1}10]$, respectively. A three-dimensional view is shown in (c).

scope of the present investigation.

LEED and scanning tunneling microscopy (STM) may have difficulty in distinguishing P and S atoms on surfaces with partial (S,P) coverages as in, say, Figs. 2(d)–2(i), while CL spectroscopy would have no such difficulty since S-2*p*

and

P-2*p* excitations are well separated. A stringent test of the (2×2) structure is to compare the *predicted* dimer and monomer CLE against experiment. This would distinguish it from the (1×1) structure analogous to the GaAs(001)-S,⁹ where the S atoms are at bridge sites, and from the (2×1) structure of Fig. 2(c), since they have only one type of sulfur. The core-level spectra of sulfur-treated InP(001) have been reported by other workers.^{10,11} They found evidence for more than one kind of surface S and made qualitative suggestions to account for the multiple-peak core-level spectra by invoking polysulfides, and physisorbed and chemisorbed sulfides.

In this paper, we give a quantitative, systematic, explanation of the observed core-level spectra under annealing, complementing the Raman results of Jin *et al.*² Note that in analyzing the experimental data we are not merely looking at just the few core-level shifts as the experimental input. Instead, the whole spectral profile, which contains the relative-intensity information as a function of energy, is considered. This gives a level of discrimination that would be impossible if we had considered only the core-level shifts.

For InP(001) surfaces treated with aqueous $(\text{NH}_4)_2\text{S}$, two distinct S-2*p* spin-orbit doublets are observed at low temperatures, with CLE in *excellent accord with the theoretical values* for the (2×2) structure. Thus, the (1×1) and (2×1) structures are excluded. At high temperatures, only one type of S excitation is found, in agreement with the theoretical picture. The theoretical picture and methods are exposed in Secs. II and III. Section II is devoted to the determination of the acceptable surface structures that may be reached by annealing within a small energy window close to the ground state. Section III discusses the first-principles calculation of core-level spectra and the treatment of the relativistic doublet stemming from the sulfur-2*p* spin-orbit interaction. The analysis of experimental core-level spectral profiles is presented in Sec. IV.

II. THEORETICAL PREDICTION OF STABLE SURFACE STRUCTURES

In this study, we are interested in the InP(001) surface covered with a monolayer of S atoms and its evolution under annealing. The structure of the surface atomic layers is different from that of the bulk as the atomic positions and electronic structure adjust to attain a minimum-energy configuration consistent with the existence of a surface. The theoretical prediction of the surface structure simply involves the calculation of the total energy of a sufficiently large slab of material and adjusting the atomic positions until the lowest-energy structure is obtained. In practice, in addition to the lowest-energy structure (the ground state), other structures which are stable (i.e., local energy minima), but lying above the ground state, are also uncovered by the search process. Annealing opens an energy window whereby structures other than the ground state become statistically or kinetically accessible. Another effect of annealing is to set in motion diffusion processes where surface atoms migrate towards the bulk and *vice versa*. In the InP(001)-S system, energy and entropy effects favor moving an S atom to the bulk while filling in the surface with a P atom. S atoms which have moved far away from the surface do not affect the energetics at the surface. Hence we consider *ideal* InP

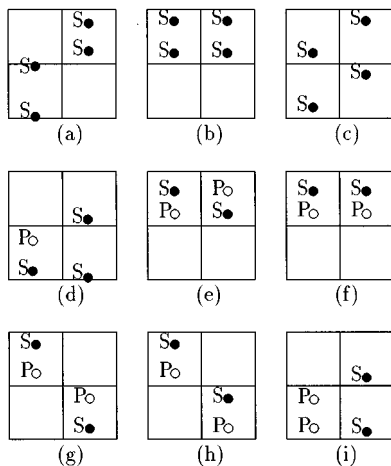


FIG. 2. (a) Top view (x - y plane) of the fully relaxed InP(001)-(S,P) surface structures. The x , y , and z axes are along $[110]$, $[\bar{1}10]$, and $[001]$, respectively. Full (1-MI-) S coverage in (a)–(c) where structure (b) is unstable; 3/4-MI-S coverage in (d); 1/2-MI-S coverage in (e)–(i).

substrates with the (2×2) -surface unit cell carrying four atoms, i.e., N_S S atoms and $(4 - N_S)$ P atoms on the surface layer. We relax the top (S,P) layer, the underlying In layer, and the next P layer in order to calculate the ground-state energies, reconstructions, as well as associated stable structures which are local minima for any given S coverage.

The prediction of the reconstructed surface structure thus depends on our ability to calculate the total energy E_T of a given system of electrons and ions. The density-functional theory (DFT) is a first-principles method for calculating E_T efficiently and with adequate accuracy. The many-electron problem is reduced to an effective one-electron problem and hence the calculation becomes similar to a Hartree self-consistent-field problem. This is, in practice, further reduced in scale by using pseudopotentials whereby only the valence electrons of the constituent ions enter into the self-consistent-field calculation. Since the core electrons are eliminated, the valence electrons can be efficiently treated using a basis set of plane waves. Needless to say, although the removal of the core electrons from the calculation is possible in the structure determination, all the electrons or some aspects of the core have to be retained (e.g., in a special pseudopotential) in the calculation of the core-level spectrum. The latter issue is dealt with in Sec. III.

The plane-wave-pseudopotential (PW-PP) calculation is implemented as follows. We use the local-density approximation (LDA) of the DFT, and nonlocal, norm-conserving, pseudopotentials.¹² The electron exchange-correlation energy is given by the Ceperley-Alder form.¹³ This DFT approach has an excellent track record of successfully predicting the structure of semiconductor surfaces,^{14–17} even with relatively low plane-wave-energy cutoffs. Reciprocal-space sampling was done using only the Γ point. The wave functions are expanded in a plane-wave basis with a 10 Ry energy cutoff. The validity of our pseudopotentials for In and P was verified earlier.¹⁷ For S, we carried out two calculations: (i) we examined the S_2 molecule and found the bond length to be 1.885 Å, in accord with the experimental value¹⁸ of 1.889 Å; (ii) we calculated the SiS molecular bond length to be 1.923 Å, also very close to the experimental value¹⁸ of 1.929 Å.

The crystal with the InP(001)-S surface is modeled as a supercell slab. The slab has six layers, each containing four atoms. The first (topmost) layer contains four S atoms. The second layer contains four In atoms, as implied by the chemistry of these materials. Subsequent layers follow in the zincblende structure, except the bottom one, which consists of four In atoms and two H atoms positioned in a (1×2) pattern to saturate the dangling bonds.¹⁷ The atoms in the bottom three layers are held fixed in their bulk InP positions, while the other atoms are relaxed to minimize the total energy. Periodic boundary conditions are applied in the x , y , and z directions. A vacuum region of width 7.225 Å—equivalent to five bulk In–P interplanar distances—is used along z , i.e., normal to the surface. For the fixed layers we used the theoretical bulk lattice constant¹⁷ of 5.78 Å which compares with the experimental¹⁹ value of 5.87 Å and the theoretical value of 5.678 Å of Alves *et al.*²⁰

The fully relaxed ground state was obtained for the (2×2) reconstructed structure depicted in Fig. 1. The surface layer consists of two sublayers S_t and S_b , each contain-

ing half the total sulfur. The top S sublayer, S_t , contains long (i.e., weak) dimers (essentially monomer pairs), with the S atoms positioned close to bridge sites, but displaced slightly in the $[\bar{1}10]$ direction to give an S_t – S_t bond length of 3.82 Å. The sublayer S_b , in contrast, contains S pairs strongly dimerized along the $[\bar{1}10]$ direction, with a bond length of 2.14 Å. The sequence of atomic planes (“sap”) in the z direction, with S_t at the surface, may be presented as

$$\text{sap} = (\text{In-P})_{\text{bulk}} - \text{In} - \text{P}_b - \text{P}_t - \text{In} - \text{S}_b - \text{S}_t. \quad (1)$$

The interplanar distances near the surface can be compared with the bulk In–P distance d_0 of 1.445 Å. The S_t layer relaxes only 0.116 Å towards the bulk, while S_b is displaced 0.335 Å below the S_t layer. The In layer below S_b remains integral while relaxing inwards but the following P layer splits to form two sublayers. The interplanar distances, starting from the leftmost In atom in (1) are In– P_b = 1.321 Å, while In– P_t = 1.532 Å, giving an average In–($P_{b,t}$) distance of 1.427 Å. The other distances are P_t –In = 1.299 Å, In– S_b = 1.169 Å, and In– S_t = 1.388 Å.

The surface loses its (1×1) periodicity and presents a (2×2) pattern, with each short dimer surrounded by four long dimers and *vice versa*. We also recovered our ground state in a larger supercell with eight atoms per plane (x dimension doubled; see also Ref. 17) and in calculations using somewhat higher-energy cutoffs. The (2×1) reconstruction (where the two types of dimers are arranged in a row) is a *local* energy minimum, about 0.21 eV per (1×1) cell above the ground state. There are other stable structures (local energy minima) for this fully S-covered surface, but lying substantially higher in energy. Such structures, including the (2×1) phase, turn out to be irrelevant to our annealing study (which extends to a temperature of about 700 K) since other structures associated with partial S coverage arising from the exchange of S with P atoms (migrating from the bulk) come into play.

The migration of surface sulfur atoms to the bulk, and bulk phosphorous atoms to the surface, are kinetically controlled processes which cannot be usefully dealt with using total-energy methods alone. Instead, we consider each mixed phase and determine the possible structures. Hence we consider *ideal* InP substrates with a monolayer of N_S S atoms and $(4 - N_S)$ P atoms on the (2×2) surface. Clearly, within this scheme, we can only study full coverage, $c = 1$, and $c = 3/4$, $1/2$, and zero. We exclude zero coverage as exploratory calculations have shown that bigger unit cells—at least a (2×4) —are needed for an adequate study of this case.

Figure 2 shows schematically a sequence of structures that were obtained by minimizing the energy with relaxation of the nuclear positions, as already described above. Figure 2(a) is the fully S covered ground-state structure of Jin *et al.* The analysis of experimental core-level spectra (see Sec. IV) shows that of all these structures, the structure of Fig. 2(e) is the one relevant to the dynamic equilibrium which exists under the 700 K anneal conditions. Figure 3 shows this half-S-covered structure in more detail.

The S–P bonds are strong, with a bond length of 2.23 Å. The P atoms “stick out” of the surface, being on a plane which is 0.24 Å above the plane of the two sulfur atoms. Given the fact that S and P atoms have nearly the same

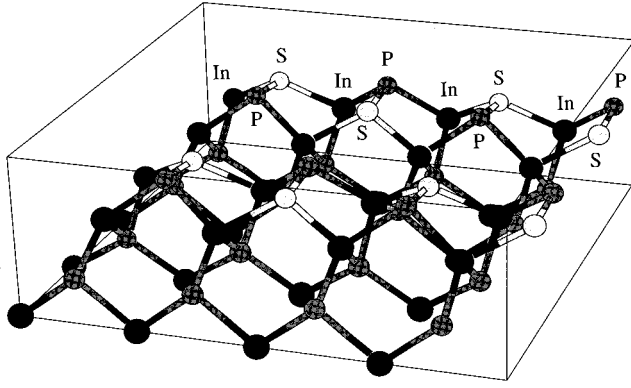


FIG. 3. A detailed view of the structure of Fig. 2(e) at half-sulfur coverage.

electron scattering cross sections, it would be easy to fail to distinguish between them in a LEED experiment; the structure would then seem to be a (2×1) reconstruction.

The relative ground-state energies of the structures shown in Fig. 2 are given in Table I. That is, for example, for coverage $c = 1/2$, we considered five possible structures, (e)–(i) in Fig. 2; we give, for each, the energy with respect to the lowest-energy structure at the same coverage, (e) in this case. In this study, we do not attempt to compare the lowest-energy structures at different coverages since that would re-

TABLE I. CL excitation energies ε_{2p} (eV) for the InP(001)-(S,P) covered surfaces displayed in Fig. 2. The ground-state energies ΔE_g per (2×2) cell (eV) are relative to the lowest-energy structure at each coverage. S* is the atom with the $2p$ core hole.

| Configuration | Remark | ε_{2p} or (ΔE_g) |
|--------------------------|--------------|--|
| <i>Full S coverage</i> | | |
| Fig. 2(a) gr. state | 2×2 | (0.0) |
| S*-S | monomer | 161.9 |
| S*-S | dimer | 162.9 |
| Fig. 2(b) unstable | 2×1 | (0.86) |
| Fig. 2(c) | 2×1 | (0.30) |
| S*- | monomerlike | 161.6 |
| <i>3/4-Ml-S coverage</i> | | |
| Fig. 2(d) | two S types | (0.0) |
| S*-P | dimerlike | 161.3 |
| S*-S | monomerlike | 160.6 |
| <i>1/2-Ml-S coverage</i> | | |
| Fig. 2(e) | 2×2 | (0.0) |
| S*-P | dimerlike | 162.9 |
| Fig. 2(f) | 2×1 | (0.17) |
| S*-P | dimerlike | 163.6 |
| Fig. 2(g) | 2×2 | (0.135) |
| S*-P | dimerlike | 163.0 |
| Fig. 2(h) | 2×2 | (0.046) |
| S*-P | dimerlike | 162.8 |
| Fig. 2(i) | 2×2 | (1.0) |
| S*-S | monomerlike | 161.6 |

quire us to address the issue of how the sulfur atoms which migrate to the bulk arrange themselves. That is, comparison of the mixed phases in an absolute sense is not attempted here. This is however not a difficulty since the annealing process will generate a dynamic equilibrium at each anneal temperature to give a specific coverage; what we need to know is the most likely near-surface structure at that coverage. Thus, for example, Table I shows that the most likely structure at $c = 1/2$ is the structure of Fig. 2(e), shown in more detail in Fig. 3.

Table I gives the “sequence of structures” arranged in order of increasing total energy. Thus for $c = 1/2$, this is (e), (h), (g), (f), and (i). This sequence was obtained from our PW-PP calculations. We repeated the calculations without using the PW-PP approach, but using a full-potential scalar-relativistic²¹ approach (FP-SR) which explicitly includes the core electrons. That is, we took the structures (nuclear positions) given in Fig. 2 and determined the total energies using the FP-SR code. We obtained the same energy sequence, and the same energy differences (to within 0.1 of an eV), thus mutually confirming the PW-PP calculations and the FP-SR calculations. Thus, for instance, the energy difference between the structures (e) and (g) in Fig. 2 is found to be 0.135 eV from the PW-PP code while the FP-SR code gives an energy difference of 0.08 eV. The energy differences ΔE_g given in parentheses in Table I are from the PW-PP calculation.

III. CALCULATION OF THE CORE-LEVEL EXCITATION ENERGIES

Using the relaxed structures provided by PW-PP structure optimization, FP-SR calculations²¹ are invoked in order to determine the sulfur- $2p$ CL spectrum. These do not use plane-wave expansions or pseudopotentials. Thus no “frozen-core” assumptions or pseudopotentials are used although such methods have been used with success.^{22–25} In the core-level-excitation process, an electron in a core level (here, the $2p$ level of sulfur) is knocked out by an incident photon and placed in an outgoing electron state. The “hole” left behind by the electron has an effective positive charge which interacts with the remaining atomic and band electrons, as well as with the outgoing electron. Thus, the photoionization process involves electronic relaxation effects in the initial state as well as in the final state which carries the outgoing electron. In most photoionization experiments, the time scale of the relaxation is short and electronic relaxation has occurred by the time the kinetic energy of the outgoing electron is measured. Hence the measured core-level excitation energy involves initial-state as well as final-state relaxation effects; in our calculations, both are properly included.

We consider a photoemission experiment where the photon energy is $h\nu$, while the energies of the initial and final states of the crystal are E_i and E_f . Then the measured kinetic energy E_{ke} of the photoelectron is such that $h\nu = E_f - E_i + E_{ke}$. Thus the measured $2p$ -CLE, $\varepsilon_{2p} = E_f - E_i$, is a property of the initial and final states of the crystal. It could be obtained from theory as a total-energy difference (TED) if the energies E_f and E_i could be calculated. The final state has a core hole and is not within the usual Hohenberg-Kohn-Sham formalism; however, a formal justification using a fic-

titious external potential may be attempted. In practice, we have found that the self-consistent process converges to an energy minimum if the core hole is in one of the deep core levels (e.g., $n = 1$ or 2) of an atom but not in a shallow level. A rigorous treatment for shallow levels will be omitted as this problem does not arise in the $S-2p$ core-hole calculations reported here.

In metals and plasmas,²² the relaxation involves the “shake up” of the Fermi sea but there is good screening. In semiconductors, the core hole is not screened out rapidly. However, if E_F is fixed by dopants in the semiconductor, then the final state containing the core hole remains neutral by an adjustment of the surface electron density.²³ The neutrality of our simulation cell in the presence of a core hole was ensured by placing an electron in the first unoccupied surface state closest to E_F , with the Fermi energy pinned at the ground-state value. In practice, all that is necessary is to place an electron in an excited state and the self-consistent energy-minimization process will bring down the electron to the first unoccupied state (a surface state) closest to the Fermi energy. (The minimization process would seek to place the electron in the core-hole itself, but it is prevented from doing this as we *impose* the existence of a hole in the $2p$ core level).

Since the eigenvalues of a Hamiltonian are the excitation energies, one may expect the CLE to be the initial-state $2p$ eigenvalue. This is not so, not only because Kohn-Sham eigenvalues are not excitation energies, but also because, as already discussed, the initial Hamiltonian changes during photoionization to include electron–core-hole interactions. The evaluation of these effects *via* many-body methods, e.g., in excitonic and x-ray edge problems,²⁶ photoionization,²⁷ etc., is numerically quite demanding. The use of model molecules or clusters²⁵ to obtain relaxation energies is not always applicable and requires rescaling from the cluster to the actual situation and hence may introduce some additional assumptions. A method that can provide a complementary estimate of the CLE is the “Slater transition-state” method (STS).²⁸ It is numerically simple and is closely related to density-functional methods. In STS, the $2p$ core-hole energy includes both initial-state and final-state effects, and is shown (under certain assumptions) to be equal to the $2p$ eigenvalue of the “transition state,” a state having a *half-occupied* core hole. Charge neutrality of the simulation unit cell is easily imposed in the semiconductor by having half an electron in the core hole and half an electron in the first available surface state just above the Fermi energy.

In the structure-relaxation calculations described in the previous section, we used a simulation slab which had six layers, with the top layer containing four S atoms and the bottom layer containing two hydrogen atoms so as to saturate the dangling bonds. Under reconstruction, the six-layer system became the eight-layer system shown in Eq. (1) when we count the split layers individually. In the CLE calculation, the surface states of the spurious H atoms were an unnecessary complication. Further, it was necessary to ensure that the bottom surface hydrogen had no uncompensated interactions with the surface sulfur when a core hole was created. Hence, for these calculations, we used a simulation slab containing *two* free surfaces containing sulfur, equivalent to a 15-layer slab (where the split layers are counted indepen-

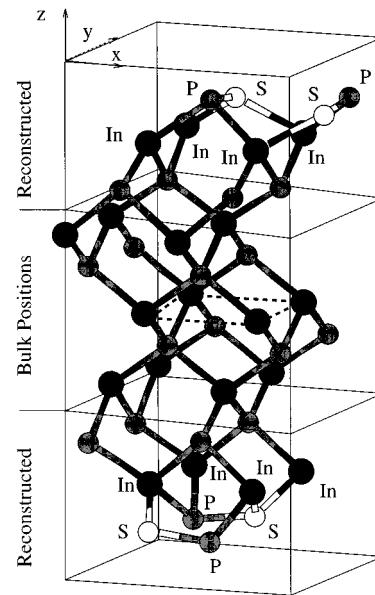


FIG. 4. A detailed view of the 15-layer slab with two-sulfur surfaces treated as a symmetrized seven-layer slab. The four In atoms joined by dashed lines form an improper mirror plane as explained in the text.

dently). This 15-layer slab can be treated as two seven-layer slabs joined through a single “mirror layer” with a $\pi/2$ rotation in the middle (Fig. 4). In Fig. 4, the mirror layer is the plane containing four bulklike In atoms connected by the dashed lines. The seven-layer slab for the structure being studied, say Fig. 2(e), i.e., Fig. 3, sits above the plane. The seven layers below the mirror plane are generated by imposing the improper operation $S_4(xyz) = (y, -x, -z)$ (about the z axis through one of the In atoms in the plane) to all atoms in the upper slab.

The above symmetrization was used to reduce (considerably) the computational scale of the problem. The zincblende structure does not lend itself to a straightforward reflection-symmetry simplification. However, the artifice used here preserves all the geometrical and chemical environments of all the atoms except the four In atoms in the central mirror layer. Even here the changes in the local environments are minimal. The consequences of having a mirror layer on the calculated electronic structure are much less objectionable than the presence of the H-atom surface states. Five vacuum layers were used to convert the 15-layer slab into a periodic supercell in the z direction.

We have calculated the $S-2p$ CL spectra of InP(001)-(S,P) surfaces using the TED method as well as with the STS method, which uses the half-occupied $S-2p$ Kohn-Sham eigenvalue. The excitation energies obtained by the TED method are probably more accurate than the STS results. The difference in the estimates from the two methods provides a theoretical “error bar” and gives a CLE uncertainty of ± 0.5 eV, even though the numerical *precision* is easily an order of magnitude better. That numerical precision justifies sharper comparisons between similar structures. The theoretical $S-2p$ excitation energies (from TED) are reported in Table I; the S atom with the core hole is marked S*. Two different spectra are expected in structures with two in-

equivalent S atoms. Further, each S-2*p* level is a relativistic doublet and hence each spectrum is expected to show a double-peak structure. The theory of the chemical shift of the relativistic doublet is discussed below.

A. The S-2*p* relativistic doublet

The S-2*p* levels are split by the spin-orbit (so) interaction to form $j = 1 \pm 1/2$, i.e., the $j = l + s$ doublets. The so splitting was included in the calculations using the method of Koelling and Harmon.²⁹ The PW-PP code is of no use for this part of the problem. Instead, we use the all-electron FP-SR-LDA code,²¹ where the spin *s* and the orbital state *l* are treated as good quantum numbers. The main code yields the self-consistent potential *V*(*r*) inside the atomic sphere, which determines the core states. The so interaction is

$$H_{so}(r,s) = \xi(r) \tilde{l} \cdot \tilde{s}, \quad (2)$$

$$\xi(r) = (\alpha^2/2)(1/r)[dV(r)/dr], \quad (3)$$

where \tilde{l} and \tilde{s} are the orbital and spin angular momentum operators, and α is the fine-structure constant. The one-electron so energy resulting from first-order perturbation theory involves the matrix-element $\langle nl | H_{so}(r,s) | nl \rangle$. Then we have

$$E(j)_{so} = \langle R_{nl} | \xi(r) | R_{nl} \rangle (j \pm 1/2)/2, \quad (4)$$

where R_{nl} is the radial function with quantum numbers *n*, *l* provided by the main full-electron code. It should be noted that both the small and large components of the wave function rendered by the scalar-relativistic calculation are included as usual in evaluating the mean values.

The calculated so splitting is 1.29 eV ($\Delta\epsilon = -0.86$ eV for $j = 1/2$ and $+0.43$ eV for $j = 3/2$). The two peaks of the doublet have intensities 1:2 since the level degeneracies are $2j + 1 = 2$ and 4.

B. Line shape

CLE contain large Madelung contributions sensitive to surface disorder. Disorder has a “smearing effect” which reduces the differences between inequivalent chemical environments of the surface atoms. Thus, the experimental CL shifts are expected to be *smaller* than that calculated for the fully ordered structure. Surface disorder has an effect on the line shape of the CL excitation by inhomogeneous broadening, etc. A theoretical calculation of the CL-excitation line shape would require a Zangwill-Soven²⁷-type treatment as well as a convolution with inhomogeneous broadening effects. In this study, we simply assume that the net effect is to yield a Lorentz-Gauss (Voigt) profile and no attempt will be made to provide a first-principles spectral line shape. This means that each *relativistic doublet* will have a line shape described by two fit parameters. However, the relative intensities of the two peaks in the doublet are determined by the degeneracies $2j + 1$, as discussed above.

IV. DISCUSSION OF THE EXPERIMENTAL SPECTRA

Photoelectron-spectroscopy measurements were carried out at the Stanford Synchrotron Radiation Laboratory using a

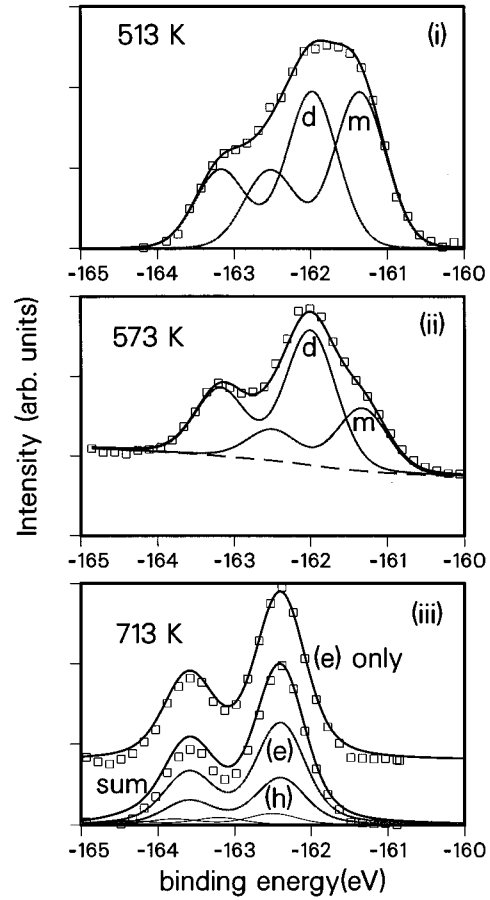


FIG. 5. Core-level spectra of InP(001)-(S,P) showing the peak structure obtained by fitting Voigt profiles. (i) Experimental data (squares, every 5th data point shown) for the surface at 513 K. The calculated spectrum (smooth curve) is the sum of CL spectra for S dimer (*d*) and S monomer (*m*) of Fig. 2(a). (ii) Experimental spectrum at 573 K. Here the intensity of *d* and *m* were *not* assumed equal in “decomposing” the spectrum. The electron background (not shown in the other panels) is also shown (dashed line). (iii) Experimental spectrum at 713 K, compared with the thermally weighted “sum” of theoretical spectra of Figs. 2(e)–2(h). Only (e), (h), and sum are labeled. The upper (displaced) curve is the theoretical spectrum for the structure of Fig. 2(e) alone.

6 m toroidal-grating monochromator beamline. The photoelectrons were collected by an angle-integrated double-pass cylindrical-mirror analyzer in a UHV chamber. The sulfur-2*p* core electrons were excited by 190 eV photons with a take-off angle of 45°. Indium-4*d* and phosphorous-2*p* core levels were also recorded and found to be identical to those reported earlier.⁴ These will not be discussed here. The samples were prepared by treating the InP material with hot (65 °C) ammonium sulfide solution to remove native oxides and attach sulfur onto the surface. The surface was again treated with fresh, room-temperature ammonium sulfide solution to dissolve physisorbed sulfur, SO₂, etc., and blow-dried with nitrogen. The experimental spectra are shown as squares in Fig. 5, where panels (i), (ii), and (iii) are for CL spectra determined at 513 K, 573 K, and 713 K. The temperature values are correct to $\pm 50^\circ$. Panel (ii) shows the electron-scattering background not shown in the other panels. The zero of the energy measurement is uncertain by a

few eV, but profile fitting (see below) using theoretical inputs overcomes this problem.

Since Fig. 2(a) is theoretically the most likely structure, we analyze the lowest temperature experimental data as follows. Monomer (m) and dimer (d) S contribute equally to Fig. 2(a). Hence we expect two equal-intensity doublets, having the same so splitting, line shape, and a 1:2 intensity ratio in each doublet. We impose these strong constraints and fit the experimental profile with two doublets (four Voigt profiles) whose peak positions are adjusted from the theoretical values only to within the expected error of ± 0.5 eV. Since the intensity is arbitrary, the calculated spectrum is scaled at one of the peaks to the experimental profile. The resulting fitted peak positions are designated the *experimental* peak values. The experimental so splitting is 1.18 eV; this will be used in displaying other data.³⁰ On fitting the experimental data at 513 K, typical of the “low-temperature spectrum,” the $2p$ experimental binding energies of d and m sulfur were -162.57 and -161.95 eV, comparing very well with the theoretical values of -162.9 and -161.9 ± 0.5 eV for the structure of Fig. 2(a). We also examined unconstrained fitting to other peak distributions, but the best fits yielded four Gauss-Lorentz peaks as before. In Fig. 5(i), the contributions from $2p$ excitations of the d and m sulfur to the total spectrum are also displayed. Given the effect of surface disorder, etc., the experimental spectrum at 513 K is in close agreement with that predicted from the (2×2) structure of Fig. 2(a), i.e., Fig. 1.

Our d peak corresponds to what Chassé *et al.*¹¹ call a “polysulfidic S . . . in a terminal position,” while our m peak (their S2) is what they attribute to “sulfur atoms in phosphorous sites in the uppermost surface” or to an In_2S_3 environment (*N.B.*, the species called “S1” by Chassé *et al.* does not occur in the temperature regime studied by us, in agreement with them). Finally, the (2×2) structure is consistent with the Auger data of Chassé *et al.*,¹¹ where d is “polysulfidic,” while m is similar to S in an In–S environment, and provides a fully quantitative analysis of the CL experiments.

On heating, other configurations begin to compete with the $T = 0$ K ground state. The next stable, fully S-covered structure is Fig. 2(c). This structure gives a single S- $2p$ CLE calculated to be ~ 161.6 eV, i.e., near the previous monomer peak. If this is formed on heating, the “dimer” intensity should decrease while the monomer peak grows. Actually, several aspects of the evolution of the surface under annealing are somewhat counter intuitive. Figure 5(ii) shows that the *monomerlike* S peak has decreased in intensity. Thus the structure of Fig. 2(c) does not form, because of other competing processes. Such a process is the surface-S \leftrightarrow bulk-P exchange. In fact, there is strong evidence for such exchanges from x-ray photoelectron diffraction studies.³¹

The 3/4-ML S-covered structure, Fig. 2(d), is particularly interesting. When a monomer S atom in Fig. 1(a) is replaced by a P atom and relaxed to minimize the energy, the initially long S–P bond contracts to form a tight S–P molecule while the dimer S–S elongates to a monomer pair. Here the S \leftrightarrow P exchange involves dimer dissociation and S–P molecular association. The *surface* rearrangement leading to Fig. 2(d) for 3/4-ML-S coverage is not seen, probably due to faster S \leftrightarrow P exchanges leading, instead, to 1/2-ML-S sur-

faces. The stable 1/2-ML-S surfaces are shown in Figs. 2(e)–2(i). In all these, the S–P molecules are tightly bound and *buckled* with the P atom projecting out. Unlike Fig. 2(a), any one of these structures, having only one kind of S atom, will produce a *single* core-level doublet spectrum.

However, the data analysis says more. The structures are close to each other in energy and contribute to the surface partition function. If we assume that all possible structures at a given coverage contribute to the surface, each structure of energy E_g would have a weight of $Z^{-1} \exp(-E_g/k_B T)$ with Z^{-1} the normalization. Such a weighted-sum theoretical spectrum for the structures of Figs. 2(e)–2(i) at 713 K is displayed as “sum” in Fig. 5(iii). The CL spectrum from Fig. 2(e) *by itself*, or (h) by itself, agrees better with experiment than the sum. Thus, contrary to “simple intuition” the annealed surface is *not* a simple weighted sum of the possible structures. Instead, the lowest-energy structure at this coverage, Fig. 2(e), is a somewhat better fit to the data. One could imagine that the lowest energy structure nucleates first and determines further surface growth (a kinetic process), and thus upsets the simple picture of thermal statistics. Further, the 1/2-ML-S-covered structure of Fig. 2(e) is also the best choice as it is consistent with LEED (2×1) data from annealed samples,⁷ since S and P atoms could look alike under LEED. The data analysis suggests that kinetic effects are relevant. Hence we have not tried a structural analysis of the spectrum of Fig. 5(ii). Structures containing sulfur atoms substituted in sites on several subsurface P planes may be relevant at these intermediate situations. Thus, at this intermediate temperature we simply find the best-fit pair of doublets where the intensities, peak positions, and linewidth parameters were optimized (without assuming equal intensity doublets). The resulting decomposition is shown in panel (ii) and fits in with the S \leftrightarrow P exchange-driven annealing scenario discussed so far.

V. CONCLUSION

In summary, we have used theoretical predictions and experimental CL spectroscopy *in tandem* to unravel the evolution of the fully-S-covered $\text{In}(001)$ -S surface to partial coverage with exchange of surface S atoms by bulk P atoms, where a delicate process of chemical association and dimer dissociation plays a determining role in structural relaxation. Studying the whole core-level spectrum (rather than just the CL shifts) provides a more thoroughgoing structure-discriminating approach. The low temperature CL spectrum is in excellent agreement with that predicted from the (2×2) reconstruction of Jin *et al.*,² while the higher temperature (~ 700 K) anneal is likely to be a surface containing one S species with rows of S–P and P–S pairs.

ACKNOWLEDGMENTS

We thank Geoff Aers and David Lockwood for many discussions and comments, Alfredo Pasquarello for a critical reading of the manuscript, and Alastair McLean for some clarifications. This work is supported by grants from the Natural Sciences and Engineering Research Council of Canada and the “Fonds pour la formation de chercheurs et l’aide à la recherche” of the Province of Québec to L.J.L. We are grateful to the “Services informatiques de l’Université de Montréal” for computer resources.

- *To whom correspondence should be addressed; electronic mail address: chandre@cm1.phy.nrc.ca
- ¹See *Synchrotron Radiation Research: Advances in Surface Science*, edited by Z. Bachrach (Plenum Press, New York, 1990); and J. Himpel *et al.*, in *Photoemission and Absorption Spectroscopy of Solids and Surfaces with Synchrotron Radiation*, edited by M. Campagna and R. Rosei (North-Holland, Amsterdam, 1990), p. 203; also, E.L. Bullock *et al.*, Phys. Rev. Lett. **74**, 2756 (1995).
 - ²J.-M. Jin, M.W.C. Dharma-wardana, D.J. Lockwood, G.C. Aers, Z.H. Lu, and L.J. Lewis, Phys. Rev. Lett. **75**, 878 (1995).
 - ³C.J. Sandroff, M.S. Hegde, L.A. Farrow, C.C. Chang, and J.P. Harbison, Appl. Phys. Lett. **54**, 362 (1989).
 - ⁴Y. Tao, A. Yelon, E. Sacher, Z.H. Lu, and M.J. Graham, Appl. Phys. Lett. **60**, 2669 (1992).
 - ⁵J. Travis, Science **262**, 1819 (1993).
 - ⁶M.P. Teter, M.C. Payne, and D.C. Allan, Phys. Rev. B **40**, 12 255 (1989).
 - ⁷C.E.J. Mitchell, I.G. Hill, A.B. McLean, and Z.H. Lu, Prog. Surf. Sci. **50**, 325 (1995).
 - ⁸C.R. Stanley, R.F.C. Farrow, and P.W. Sullivan, in *The Technology and Physics of Molecular Beam Epitaxy*, edited by E.H.C. Parker (Plenum, New York, 1985), Chap. 9.
 - ⁹T. Ohno, Surf. Sci. **255**, 229 (1991); M. Sugiyama, S. Maeyama, and M. Oshima, Phys. Rev. B **50**, 4905 (1994).
 - ¹⁰Y. Fukuda, Y. Suzuki, N. Sanada, S. Sasaki, and T. Ohsawa, J. Appl. Phys. **76**, 3059 (1994).
 - ¹¹T. Chassé, H. Peisert, P. Streubel, and R. Szargan, Surf. Sci. **434**, 331 (1995).
 - ¹²L. Kleinman and D.M. Bylander, Phys. Rev. Lett. **48**, 1425 (1982).
 - ¹³D.M. Ceperley and B.J. Alder, Phys. Rev. Lett. **45**, 566 (1980).
 - ¹⁴J. Dabrowski and M. Scheffler, Appl. Surf. Sci. **56**, 15 (1992).
 - ¹⁵M. Needels, M.C. Payne, and J.D. Joannopoulos, Phys. Rev. Lett. **58**, 1765 (1987); I. Stich, M.C. Payne, R.D. King-Smith, J.-S. Lin, and L.J. Clarke, *ibid.* **68**, 1351 (1992).
 - ¹⁶J.-M. Jin and L.J. Lewis, Phys. Rev. B **49**, 2201 (1994); J.-M. Jin, L.J. Lewis, V. Milman, I. Stich, and M.C. Payne, *ibid.* **48**, 11 465 (1993).
 - ¹⁷J.-M. Jin and L.J. Lewis, Surf. Sci. **325**, 251 (1995).
 - ¹⁸D.R. Lide, in *Handbook of Chemistry and Physics* (CRC Press, Boca Raton, 1992), pp. 9–22.
 - ¹⁹J.C. Brice, in *Properties of Indium Phosphide* (INSPEC, London, 1991), p. 5, and references cited therein.
 - ²⁰J.L.A. Alves, J. Hebenstreit, and M. Scheffler, Phys. Rev. B **44**, 6188 (1991).
 - ²¹M. Methfessel, Phys. Rev. B **38**, 1537 (1988); M. Methfessel, D. Hennig, and M. Scheffler, *ibid.* **46**, 4816 (1992), and references therein.
 - ²²F. Perrot and M.W.C. Dharma-wardana, Phys. Rev. Lett. **71**, 797 (1993); A. Rosengren and B. Johansson, Phys. Rev. B **22**, 3706 (1980).
 - ²³E. Pehlke and M. Scheffler, Phys. Rev. Lett. **71**, 2338 (1993).
 - ²⁴X. Blase, A.J.R. de Silva, Xuejun Zhu, and S.G. Louie, Phys. Rev. B **30**, 8102 (1994).
 - ²⁵A. Pasquarello, M.S. Hybertsen, and R. Car, Phys. Rev. Lett. **74**, 1024 (1995).
 - ²⁶G.D. Mahan, *Many-Particle Physics* (Plenum, New York, 1990), Chap. 8.
 - ²⁷A. Zangwill and P. Soven, Phys. Rev. A **21**, 1561 (1980).
 - ²⁸J.C. Slater, *The Self-Consistent Field for Molecules and Solids* (McGraw-Hill, New York, 1974), Vol. IV; R.M. Dreizler and E.K.U. Gross, *Density Functional Theory* (Springer-Verlag, New York, 1990), Sec. 4.4.
 - ²⁹D.D. Koelling and B.N. Harmon, J. Phys. C **10**, 3107 (1977).
 - ³⁰This is equivalent to fixing the value of λ in $-\lambda \mathbf{L} \cdot \mathbf{S}$ in the so term (Ref. 24).
 - ³¹Z.H. Lu and R. Cao (unpublished).